Journal of Chromatography, 363 (1986) 1–30
Elsevier Science Publishers B.V., Amsterdam — Printed in The Netherlands

CHROM. 18 649

FRAMEWORK FOR MAXIMIZING THROUGHPUT IN PREPARATIVE LIQUID CHROMATOGRAPHY

JOHN H. KNOX*
Department of Chemistry, University of Edinburgh, West Mains Road, Edinburgh, EH9 3JJ (U.K.)
and
HAZEL M. PYPER
Huntingdon Research Centre, Huntingdon, Cambridgeshire (U.K.)

SUMMARY

This paper addresses the questions: (a) Should one use volume or concentration overloading or both to achieve maximum throughput in preparative liquid chromatography? (b) Is the plate height concept valid for overloaded columns? (c) What are the main factors limiting throughput? (d) What column lengths, L, and particle diameters, d_p, provide maximum throughput?

We conclude (a) that concentration overloading will always provide the greatest throughput but that the injected sample volume may be a substantial fraction of the volume of the eluted peak, (b) that peak widths increase as the square root of the distance migrated under concentration overload and that the plate height concept can be used in optimisation calculations, (c) that the major restriction on throughput is the minimum number of theoretical plates, N^*, required to achieve adequate resolution of solutes being isolated, (d) that maximum throughput is achieved for a specific ratio d_p^2/L determined by N^* and other operating parameters.

In practice for N^* values between 2000 and 50 we are likely to use columns 200–2000 mm long packed with 10–60 μm diameter particles giving throughputs between 0.1 and 20 g/h per cm^2 of column cross section at a capacity ratio of 4.

INTRODUCTION

Preparative liquid chromatography (PLC) is distinguished from high-performance liquid chromatography (HPLC) not so much by its scale as by its purpose. PLC may be defined as LC carried out for the purpose of isolating purified chemical substances, whereas analytical LC or HPLC is carried out for the purpose of identifying and quantifying the components of mixtures. The scale of PLC is normally larger than that of HPLC but per run may nonetheless range from micrograms to grams. Production liquid chromatography, for which we shall also use the acronym PLC, can be defined as LC carried out for the purpose of commercial production and differs from preparative LC in that the cost element now becomes all-important. Its scale will normally be within the range of milligrams to kilograms per run.

0021-9673/86/$03.50

In nearly all practical cases PLC will also be associated with column overloading since a maximum throughput within stated limits of purity and yield is always desired. It is with PLC in this form that the present paper is primarily concerned.

A column is said to be overloaded when the sample injected is so large that the eluted peak is significantly wider than that resulting from the injection of an infinitesimal or analytical sample. "Significantly wider" in this context might mean 10–20% wider, indicating an increase of 20–50% in the height equivalent to a theoretical plate (HETP).

Optimisation of performance in analytical LC implies seeking conditions which combine maximum plate efficiency and minimum elution time, under the restriction of a limited pressure drop. The theory of such optimisation has been widely discussed[1–6] and leads to the specification of the optimum column dimensions, in particular optimum particle size, d_p, and column length, L, for a specified plate number, N.

Optimisation of performance in preparative LC implies seeking conditions which provide the maximum injection rate or collection rate (throughput) of material with specified purity and at specified yield, but again under the restriction of a limited pressure drop across the length of the column. Any theory of optimisation must lead to the prediction of the combinations of column length and particle diameter which lead to maximum throughput.

In what follows we shall assume that the throughput for any type of column (given length and particle size) will be proportional to its cross sectional area. Accordingly our task is to optimise the throughput per unit cross sectional area of column. We note that Hupe and Lauer[7] have considered in detail the trade-off between increasing the column length and cross section for solutes which are just resolved. We shall in general consider only the case where there is already sufficient resolution at the analytical level to allow some degree of column overloading before adequate resolution is lost.

Optimisation of performance in production LC implies minimizing the cost of production per unit volume of product with specified purity. Pressure drop and yield are no longer restrictions but can be chosen to minimize cost. This optimisation exercise is much more complex than for preparative LC as it has to include considerations of capital cost of equipment, cost of solvents and packings, cost of recycling solvents etc. Such matters will only be considered in passing.

Before embarking on the theory of optimisation of PLC, we take it as self evident that the initial step in developing any practical preparative separation will be to find the elution conditions which, under analytical loading, give the best possible α values (relative values of retention ratios) for the solutes of interest. As in optimisation of HPLC, the larger the relevant α values, the faster can a separation with given resolution be achieved, and so the greater the throughput.

PEAK MIGRATION AND RESOLUTION UNDER CONDITIONS OF OVERLOAD

There are two ways in which a column may be technically "overloaded". First, the volume of the injected sample may be so large that eluted peaks are significantly wider than those from analytical samples, although the solute concentration is low

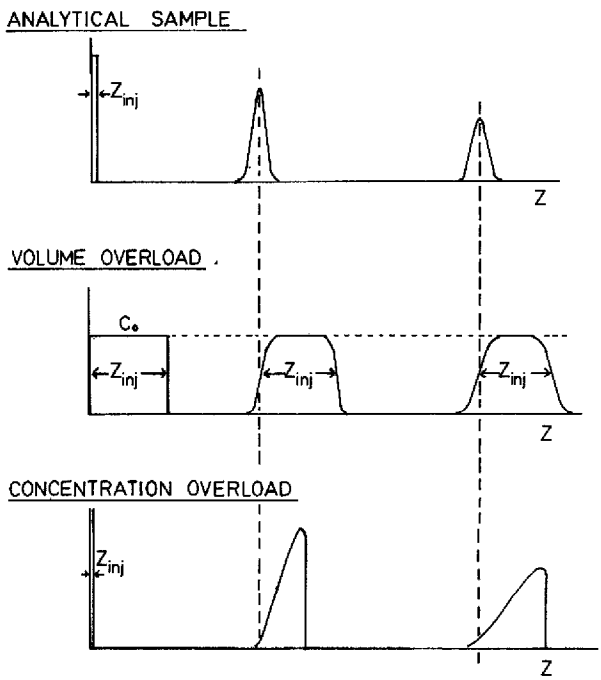

Fig. 1. Development of peak profiles during migration along a column for analytical and overload samples.

and still remains within the range of the linear part of the partition isotherm. We term such overloading "pure volume overloading".

Second, the concentration or quantity of solute injected may be so large that, even with a very small injection volume, the resulting peak is wider than that from an analytical sample. In this case the solute concentration no longer falls within the range of the linear part of the partition isotherm. Such overloading is termed "concentration overloading". Volume and concentration overloading may, of course, be combined. In such a case the width of the eluted peak may be reduced either by reducing the injected volume or by reducing the injected quantity.

Under conditions of pure volume overloading, when the injected volume is sufficiently large, eluted peaks will be flat topped, but symmetrical. Under conditions of concentration overloading peaks will generally be asymmetric, normally showing sharp fronts and extended tails.

The way in which the peak of a single solute migrates along a column under analytical and overload conditions is shown schematically in Fig. 1 which plots solute concentration against distance from the injection point at different stages in elution.

The peak concentration–distance profile for an analytical injection follows the well known Gaussian equation

$$C = \frac{Q}{\sqrt{2\pi H_0 z}} \exp\left[-\Delta z^2/2H_0 z\right] \tag{1}$$

where C is the total concentration of solute within the column at a distance z from

the column inlet measured as quantity per unit volume of the packed bed, Q the quantity of solute injected per unit area of column, H_0 the plate height for an infinitesimal sample, z the distance migrated by peak maximum and Δz the distance measured from peak maximum.

When a similar low concentration of solute is injected but the injection volume is large, the peak profile is represented by[8-11]

$$C = \frac{Q}{2\,z_{\mathrm{inj}}}\left\{\mathrm{erf}\left[\frac{\Delta z}{\sqrt{2H_0 z}}\right] - \mathrm{erf}\left[\frac{\Delta z - z_{\mathrm{inj}}}{\sqrt{2H_0 z}}\right]\right\} \tag{2}$$

where z_{inj} is the width of solute band within the column (assumed rectangular in profile) immediately following its injection. The error function is defined as

$$\mathrm{erf}\left[\frac{X}{\sqrt{2}}\right] = \sqrt{\frac{2}{\pi}}\int_0^X \exp\left[-\frac{x^2}{2}\right]\mathrm{d}x \tag{3}$$

z_{inj} is related to the volume of sample injected, V_{inj}, by

$$z_{\mathrm{inj}} = V_{\mathrm{inj}}/A_{\mathrm{m}}\,(1 + k) \tag{4}$$

where A_{m} is the cross section of eluent phase within the column bed and k the column capacity ratio of solute (note: k will be used in place of k' in order to simplify the writing of equations). The total concentration within the column immediately after injection, C_0, is given by

$$C_0 = Q/z_{\mathrm{inj}} \tag{5}$$

When $z_{\mathrm{inj}} \to 0$ eqn. 2 reduces to eqn. 1.

With an analytical sample the maximum solute concentration in the band is $C_{\max} = Q/\sqrt{2\pi Hz}$ and falls in proportion to $1/\sqrt{z}$ as the band migrates whereas in the volume overload situation if z_{inj} is sufficiently large, say greater than eight standard deviations (*i.e.* $8/\sqrt{Hz}$), the peak is flat-topped and the maximum concentration remains at C_0.

Under conditions of concentration overload the situation is much more complex due to the combined effects of kinetic and thermodynamic dispersion[12]. However, when kinetic dispersion is negligible a straightforward result is obtained[13-15]. When the partition isotherm is concave to the C_{m} axis (C_{m} is the concentration in eluent) the peak has a sharp front and extended tail. The column capacity ratio corresponding to the migration of an element with a specified mobile phase concentration C_{m} in the tail of the peak is given by

$$k_{C_{\mathrm{m}}} = \frac{\mathrm{d}C_{\mathrm{s}}}{\mathrm{d}C_{\mathrm{m}}} \tag{6}$$

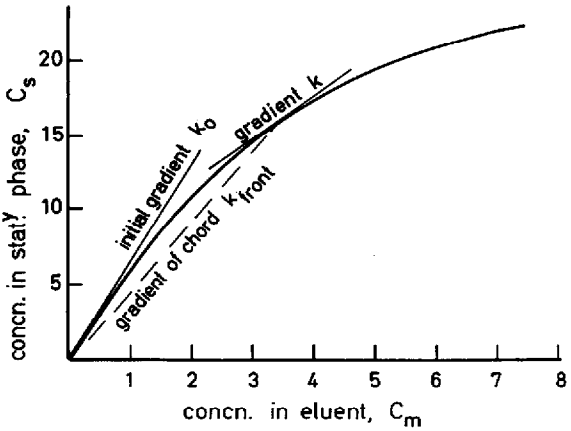

Fig. 2. Relationship between various capacity factors and the partition isotherm. k_0 = Capacity ratio of solute at $C = 0$; k = capacity ratio for a particular concentration C_m in eluent; k_{front} = capacity ratio for a front with concentration C_m.

where C_s and C_m are the concentrations per unit volume of the column bed for solute in the stationary and mobile phases respectively, so that the total concentration within the column bed, C, is given by

$$C = C_m + C_s \tag{7}$$

The column capacity ratio for the front on the other hand follows the equation

$$k_{front} = C_s/C_m \tag{8}$$

These equations are illustrated in Fig. 2.

The very complex situation which arises when band dispersion arises from both kinetic and thermodynamic effects (*i.e.* those due to non-linearity of isotherm) has been examined by Haarhoff and Van der Linde[12]. They were able to obtain an explicit mathematical expression only for the case where the partition isotherm could be written in the simple form

$$C_s = k_0 C_m (1 - \alpha C_m) \tag{9}$$

As shown later this approximates to the Langmuir isotherm at low C_m values. Their closed solution has been tested experimentally by Cretier and Rocca[16] and using computer simulation by Poppe and Kraak[17].

While the equations of Haarhoff and Van der Linde[12] are undoubtedly realistic they are somewhat complex and do not readily give guidance to the general practitioner who wishes to derive optimised conditions for a particular PLC separation. Nevertheless an important conclusion arises from their work, which has also been used by De Jong *et al.*[18], namely that if the apparent HETP is defined as the second moment of the peak divided by the column length, it is possible to a good approximation to separate the total HETP into two contributions:

$$H_{\text{total}} = H_0 + H_{\text{th}} \tag{10}$$

H_0 is the kinetic contribution to the plate height for an infinitesimal sample and H_{th} is the thermodynamic contribution arising from the non-linearity of the isotherm.

Fig. 3 illustrates the problem of peak resolution under analytical and overload conditions, and re-emphasises the importance, when optimising PLC, of initially obtaining the highest possible resolution of solutes on the analytical scale. Under pure volume overload, adequate resolution of the two solutes 1 and 2 will be maintained until the peak first eluted occupies the entire space between the two peaks. The maximum volume which can be injected before significant overlap occurs is given approximately by

$$V_{\text{inj}} = (V_{R2} - V_{R1}) - \sqrt{2\pi}\,(\sigma_1 + \sigma_2) \tag{11}$$

where V_{R2} and V_{R1} are the retention volumes of solutes 1 and 2, and σ_1 and σ_2 are the standard deviations of peaks for analytical injection of solutes 1 and 2.

If sample cutting is employed overlap may be allowed and the optimum overlap for specified restrictive conditions of purity and yield may be obtained[9,19].

With increasing concentration overload while using small injected volumes, the fronts of the overloaded peaks elute progressively earlier until the front of peak

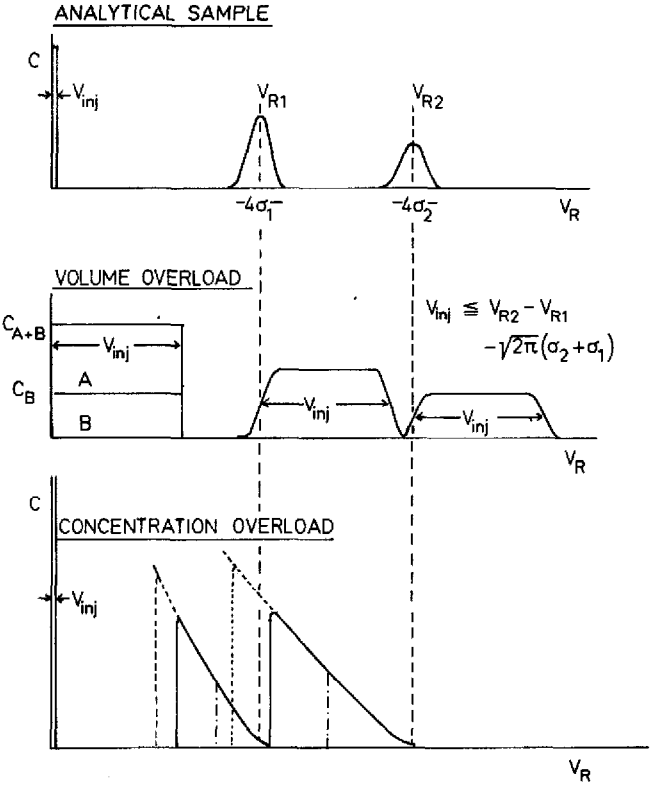

Fig. 3. Resolution of solutes 1 and 2 under analytical and overload conditions.

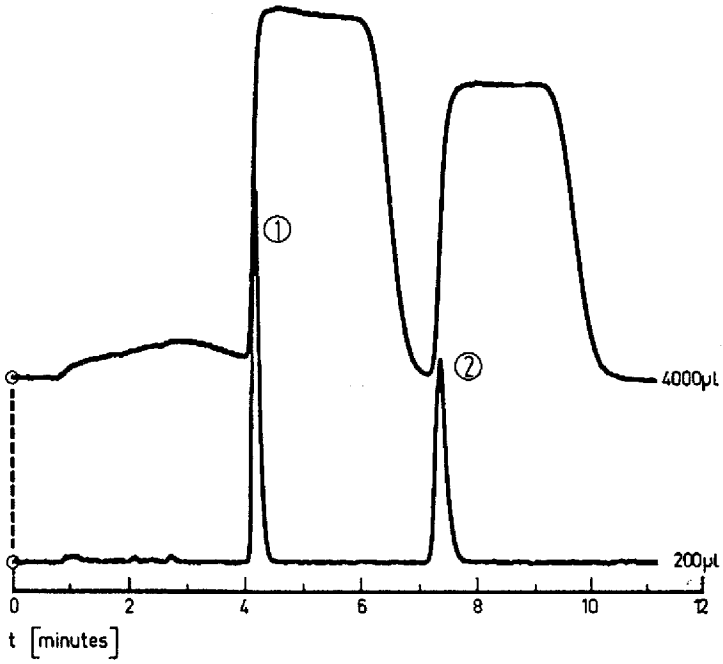

Fig. 4. Practical illustration of volume overload from Eisenbeiss et al.[20]. Solutes, pentylbenzene (1) and octylbenzene (2); injection, 200 µl containing 2.5 µg each solute (lower), 4000 µl containing 50 µg each solute (upper); column, 250 × 4 mm I.D.; packing, 7 µm LiChrosorb RP-8; eluent, acetonitrile–water (75:25, v/v); flow-rate, 1.5 ml min^{-1}; detector, UV, 254 nm, 0.04 a.u.f.s. (Reproduced by permission of the authors and of *Chromatographia.*)

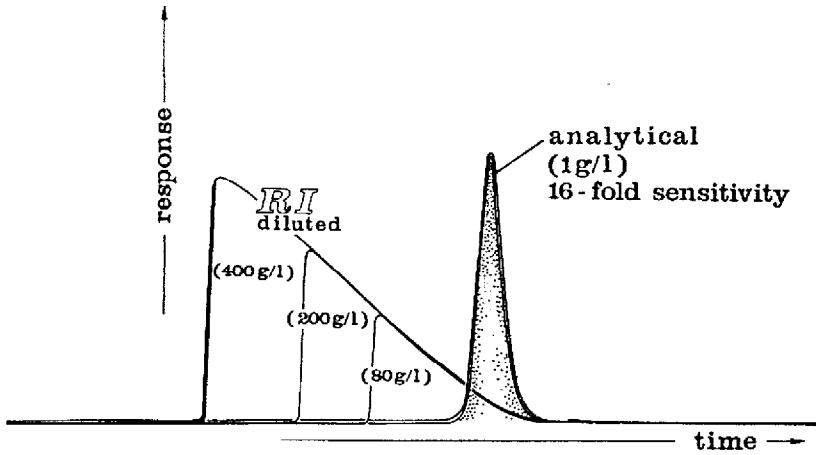

Fig. 5. Practical illustration of concentration overload from Eisenbeiss *et al.*[20]. Solute, diethylphthalate; injections, 30 µl of solutions containing 1, 80, 200 and 400 g/l; column, 250 × 4 mm I.D.; packing, 5 µm LiChrosorb SI60; eluent, heptane–ethylacetate (90:10, v/v); flow-rate, 3 ml min^{-1}; detector, refractive index with scavenging flow for overload samples. (Reproduced by permission of the authors and of *Chromatographia.*)

2 elutes at the tail of peak 1. Thereafter overlap occurs and resolution deteriorates. The optimisation of the overload when peak cutting is used can again in principle be carried out. Experimental justification of the above conclusions is provided by Eisenbeiss *et al.*[20] and is illustrated by Figs. 4 and 5 taken from their publication.

The simple picture presented in Fig. 3 shows that a higher load can always be resolved under concentration overload conditions than under pure volume overload conditions. However, the question arises as to whether a judicious combination of volume and concentration overload might not produce higher loading and throughput than concentration overload alone.

Fig. 6 addresses this question. To simplify the analysis we assume that kinetic dispersion is small and can be neglected to a first approximation. Accordingly a low concentration injection of a finite volume (pure volume overload conditions) will migrate down the column with an unchanging rectangular concentration–distance profile. A small volume injection of high-concentration solution (concentration overload situation) will migrate along the column as a tailing peak having a sharp front. For convenience we take the peak shape to be triangular as indicated by the

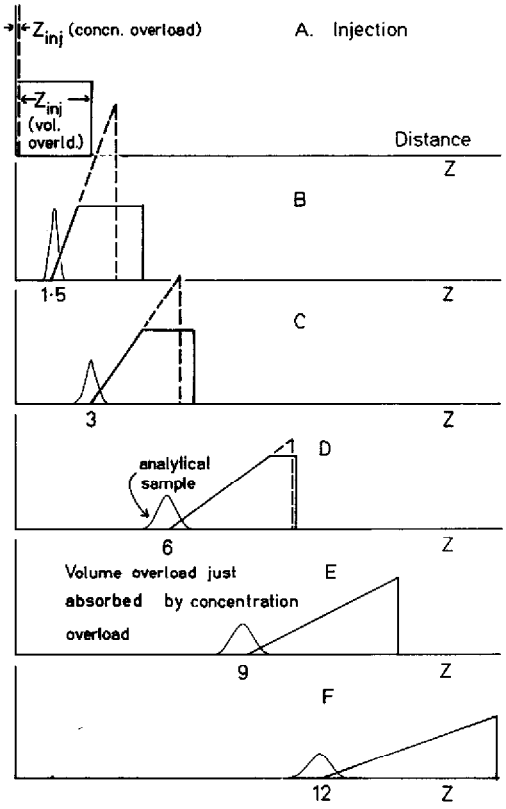

Fig. 6. Development of peak profiles for concentration overload when peak profile is triangular, and for combined volume–concentration overload showing that volume overload can be absorbed by concentration overload.

broken lines in Fig. 3. The peak shape reflects the partition isotherm as given by eqn. 6.

Since the element of eluate containing a given concentration C_m will migrate at the uniform rate given by eqn. 6, the peak shape remains constant during migration except in so far as it becomes wider in proportion to the distance migrated and at the same time is truncated on the high concentration side so that the peak area remains constant. In the case of the triangular peak shown in Fig. 6, dC_m/dz is proportional to $1/z$.

Consider now the migration of an initially rectangular concentration plug where maximum concentration lies in the overload region. Such a plug will maintain a sharp front but will develop a sloping tail as shown by the full lines in Fig. 6. This tail will coincide with the lower part of the tail of the concentration-overloaded peak containing the same quantity of solute. As the plug migrates the length of the plateau region declines. This is clearly necessary if the peak area is to remain constant but is also required by eqns. 6 and 7 and Fig. 2. They show that the migration rate of the front must be slower than the migration rate of the element in the tail having the same concentration where the isotherm is concave to the C_m axis. Eventually, as shown in Fig. 6E, the plateau disappears and the peak arising from the plug-injection has exactly the same profile as the peak arising from the small volume injection. This result is not restricted to a triangular peak as has been demonstrated by Smit *et al.*[21]. However, with a triangular peak, whose validity is justified later, the peak width at stage E is exactly twice that of the initial injection. At this stage the volume overload may be said to be absorbed into the concentration overload.

From this elementary analysis of the situation the following conclusions may be reached.

(1) The final eluted peak profile under concentration overload conditions for a given quantity of solute is independent of the sample volume up to a critical volume V^*.

(2) V^* is approximately half of the volume of the peak arising from a small volume injection, the exact proportion depends upon the shape of the isotherm.

(3) In PLC the injected volume V_{inj} may be any volume up to V^* without affecting the peak width.

(4) In determining the maximum quantity which can be injected in practice, volumes of around V^* of progressively more concentrated solutions should be injected until resolution deteriorates to the minimum acceptable value.

(5) Combination of concentration and volume overload does not increase the load which can be placed upon a column. For injection volumes up to V^* the load for a stated resolution will be independent of the injected volume. For larger injection volumes it will be less.

The main conclusion that injection volumes up to V^* have no effect on peak shape or peak width raises the question of whether one should inject small concentrated samples ($V_{inj} \rightarrow 0$) or a larger more dilute sample ($V_{inj} \rightarrow V^*$). There seem to us to be several arguments in favour of using relatively large volumes close to V^*.

(1) The key to optimising sample injection in PLC is the uniform distribution of sample over the column cross section. In this way, particularly under concentration overload conditions, the overload is uniform over the column section and the migrating band therefore has the same profile along any line parallel to the axis of the

column. A number of studies of how this can best be achieved have been published[9,22,23].

(2) Often large samples will contain minor contaminants which are permanently adsorbed at the inlet end of the column. If these are not uniformly distributed over the column section variations in the retentive power and possibly flow resistance over the top layers of the column will develop leading to deterioration in column performance with use.

(3) In general with current injection devices, uniform distribution of sample will be achieved most reliably with the largest permissible sample volume.

(4) The viscosity of a concentrated solution will normally differ significantly from that of eluent. If the viscosity of the injected sample exceeds that of the eluent and if the sample is not uniformly distributed it will form a viscous plug at the head of the column which will only slowly be absorbed into the main eluent stream. This will lead to a severely tailed elution peak. On the other hand if the injected sample is less viscous than eluent, fingering will occur again leading to peak distortion and unnecessary broadening.

We have examined the effects of volume and concentration overloading using a specially designed PLC injector and column system as described elsewhere[24]. The results confirm the above conclusions.

DISTRIBUTION ISOTHERMS AND PEAK SHAPES

In developing guidelines for optimising throughput in PLC it is particularly helpful if peaks can be approximated by triangles. In practice this is often the case when columns are overloaded[17,20,25] and a good illustration is shown by Fig. 5. It is, however, important to establish that partition isotherms which correspond to triangular peaks are in fact realistic.

The simplest isotherm which takes account of concentration overloading is the Langmuir isotherm which was originally conceived to handle adsorption on to energetically homogeneous surfaces from a liquid or gas. In chromatography, and particularly in liquid chromatography, great stress is laid on the achievement of energetically homogeneous adsorbents since such adsorbents exhibit a substantial range of concentration over which the isotherm is linear. Accordingly they give symmetrical elution peaks up to a relatively high sample loading. Since the absolute concentration of retained solute in the stationary phase is nearly always much greater than that in the mobile phase (since $V_s \ll V_m$ and k normally exceeds unity) molecular overcrowding as solute concentration increases, first occurs in the stationary phase. The Langmuir isotherm must therefore describe the *most favourable* situation which can arise in practice under overload conditions. In many cases the isotherm curvature and the change in curvature will be more severe.

Our first task is then to state the form of the Langmuir isotherm and the forms of the two idealized peaks; these are the triangular R_F peak in which the plot of concentration C_m against distance migrated is a straight line and the triangular k peak where the plot of concentration against retention time is a straight line. We use the symbols L, $R\Delta$, and $k\Delta$ to refer to these three cases. They are shown diagramatically in Fig. 7 and are represented by eqns. 12–14.

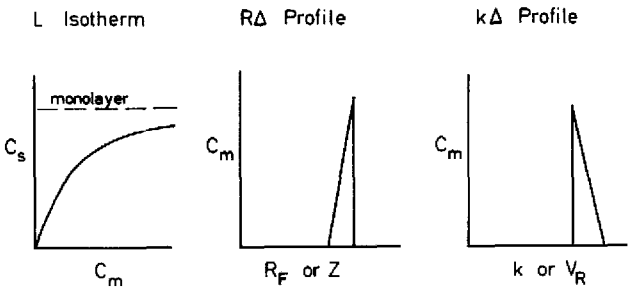

Fig. 7. Formal illustration of three possible types of distribution under overload conditions. The Langmuir distribution isotherm, the triangular R_F peak profile and the triangular k peak profile.

L Isotherm

$$C_s = \frac{k_0 C_m}{1 + \alpha C_m} \tag{12}$$

RΔ Peak

$$R_F = R_{F_0}\left\{1 + 2\left(\frac{k_0}{1 + k_0}\right)\alpha C_m\right\} \tag{13}$$

kΔ Peak

$$k = k_0(1 - 2\alpha C_m) \tag{14}$$

Isotherms corresponding to the *RΔ* and *kΔ* peak shapes are obtained using eqn. 15 which is the integral form of eqn. 6 along with eqn. 16 as required.

$$C_s = \int_0^{C_m} k \, dC_m \tag{15}$$

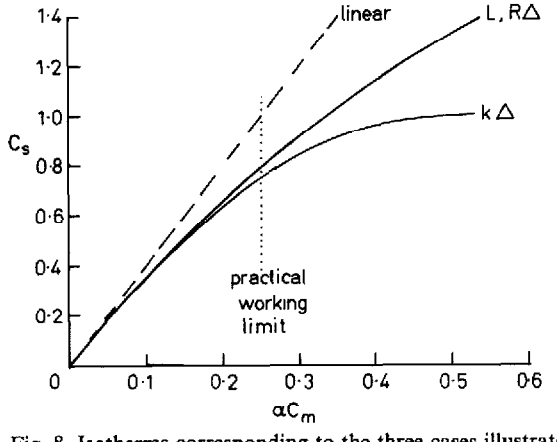

Fig. 8. Isotherms corresponding to the three cases illustrated in Fig. 7, when $k_0 = 4$ and $\alpha = 1$.

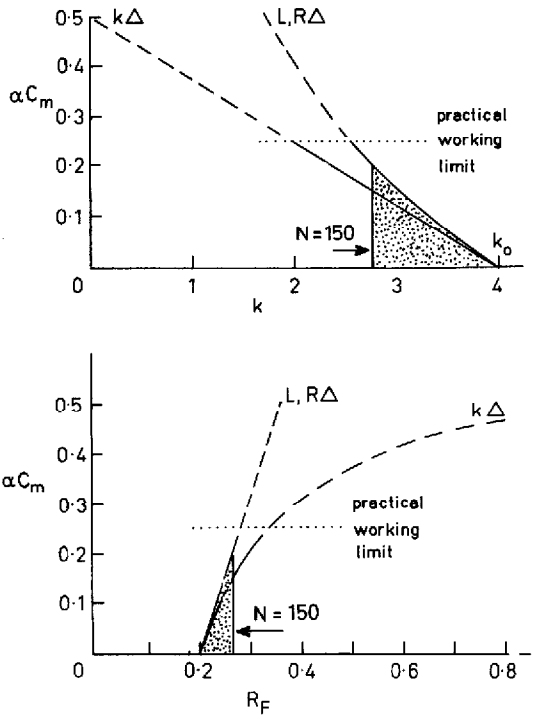

Fig. 9. Peak profiles corresponding to the three cases illustrated in Figs. 7 and 8. Plate numbers calculated on basis of eqn. 28.

$$k = \frac{1}{R_F} - 1 \qquad \text{or} \qquad R_F = \frac{1}{1 + k} \tag{16}$$

The peak shape corresponding to the Langmuir isotherm is obtained by eqn. 6 coupled with eqn. 16 as required. The mathematical manipulations are straightforward and the final results are most usefully expressed in the form of power series which enable direct comparisons to be made. The equations for the three isotherms, peak profiles on an R_F basis, and peak profiles on a k basis are given by eqns. 17–25 and illustrated in Figs. 8 and 9.

Isotherms

$$\text{L:} \quad C_s = k_0 C_m \{1 - (\alpha C_m) + (\alpha C_m)^2 - (\alpha C_m)^3 + \ldots .\} \tag{17}$$

$$R\Delta\text{:} \quad C_s = k_0 C_m \left\{1 - (\alpha C_m) + \frac{4}{3}\psi(\alpha C_m)^2 - 2\psi^2(\alpha C_m)^3 + \ldots .\right\} \tag{18}$$

$$k\Delta\text{:} \quad C_s = k_0 C_m \{1 - (\alpha C_m)\} \qquad \text{(exact)} \tag{19}$$

Peak shapes on k basis

$$\text{L:} \quad k = k_0 \{1 - 2(\alpha C_m) + 3(\alpha C_m)^2 - 4(\alpha C_m)^3 + \ldots .\} \tag{20}$$

$$R\Delta\text{: } k = k_0\{1 - 2(\alpha C_m) + 4\psi(\alpha C_m)^2 - 8\psi^2(\alpha C_m)^3 + \ldots.\} \quad (21)$$

$$k\Delta\text{: } k = k_0\{1 - 2(\alpha C_m)\} \quad \text{(exact)} \quad (22)$$

Peak shapes on R_F basis

$$\text{L: } R_F = R_{F_0}\left\{1 + 2(\psi\alpha C_m) + \left(\frac{k_0 - 3}{k_0}\right)(\psi\alpha C_m)^2 + \left(\frac{k_0 - 1}{k_0}\right)(\psi\alpha C_m)^3 + \ldots.\right\} \quad (23)$$

$$R\Delta\text{: } R_F = R_{F_0}\{1 + 2(\psi\alpha C_m)\} \quad \text{(exact)} \quad (24)$$

$$k\Delta\text{: } R_F = R_{F_0}\{1 + 2(\psi\alpha C_m) + 4(\psi\alpha C_m)^2 + 8(\psi\alpha C_m)^3 + \ldots.\} \quad (25)$$

where $\psi = k_0/(1 + k_0)$ and $R_{F_0} = 1/(1 + k_0)$.

It may be noted that all three isotherms (Fig. 8) show the same initial gradient, k_0, and initial curvature α. They differ only in the third and later terms in the bracketted polynomials. It is noteworthy that the L and $R\Delta$ isotherms have identical third terms when $k_0 = 3$ and that, for all practical LC purposes, they are identical. The $k\Delta$ isotherm deviates significantly from the other two at values of αC_m above 0.2. Similar conclusions, of course, apply to the various peak shapes (Fig. 9). Those for L and $R\Delta$ are almost indistinguishable while those for $k\Delta$ deviate significantly as αC_m increases.

It is important to note that marked deviation from the ideal peak shape is observed for quite low values of αC_m and relatively small deviations of the isotherm from linearity. Unless we are prepared to see peaks excessively widened by isotherm non-linearity, αC_m values at the column outlet must not exceed about 0.2 which corresponds, roughly speaking, to peaks spread over about one third of their elution time and so to N values of around 150. Greater peak asymmetry will, of course, occur at the start of the column. It must be noted that the maximum values of αC_m for the $R\Delta$ and $k\Delta$ peak profiles are limited since R_F cannot exceed unity and k cannot become negative. For the L isotherm αC_m may have any value since when $\alpha C_m = \infty$, $R_F = 1$ and $k = 0$. Such extreme values of αC_m are not, of course, realistic in practice and the unrealistic features of the proposed expressions need not be of concern.

RELEVANCE OF THE PLATE CONCEPT FOR OVERLOADED COLUMNS

It is often suggested that the plate concept cannot apply when eluted peaks are asymmetric or if they are broadened either by volume or concentration overload. This is incorrect. It is always possible to state that a particular column is "equivalent to a certain number, N, of theoretical plates", and we can define this number by

$$N = \left\{\frac{L}{\sigma_z}\right\}^2 \quad (26)$$

where L is the column length and σ_z^2 the second moment of peak measured in distance units within the column taken about the mean. In the same way it is possible to define the HETP by

$$H_{\text{total}} = \sigma_z^2/L \tag{27}$$

What is not legitimate is to interpret H in terms of purely kinetic phenomena. However, if the dispersions arising from both kinetic and thermodynamic effects are independent eqn. 10 can be applied. For this approach to be useful in optimisation it is desirable that both H_0 and H_{th} are more or less independent of column length. Only then can optimum column parameters be readily derived.

We must therefore examine how the peak variance or second moment arising from isotherm non-linearity develops as a peak migrates along a column.

A simplified approach is illustrated in Fig. 10 where a triangular peak (*RΔ* peak profile) migrates along a column. The quantity of solute in the mobile phase is taken as proportional to the peak area. Since the quantity in any peak as it migrates along the column is constant the area must remain constant while the peak broadens and becomes lower. The range of the isotherm which is embraced by the peak thus decreases as it migrates so the relative peak width declines. It is readily seen from the geometry of the figure that the width increases as the square root of the distance, z_0, migrated by the low concentration edge of the peak. Thus if N is measured as

$$N = q(z_0/w_z)^2 \tag{28}$$

N will increase linearly with z_0. When the distance migrated, z, is taken as other elution distances (*e.g.* that of the centre of mass of the peak or its maximum, z_{cm} or z_{max}) the plots of N *versus* z deviate slightly from the straight line plot of N *versus* z_0 as illustrated in Fig. 10.

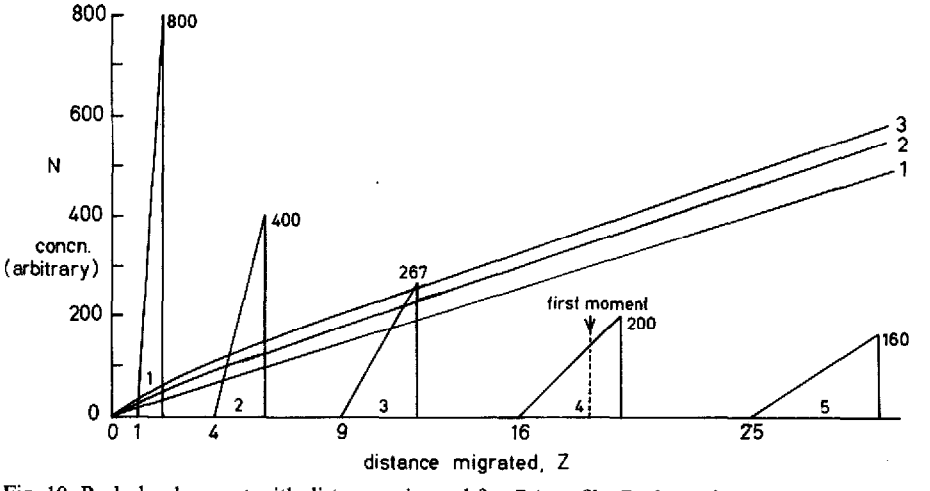

Fig. 10. Peak development with distance migrated for *RΔ* profile. Peak maximum concentrations shown on each peak. Lines are plots of N *versus* distance migrated calculated according to the formulae $16(z_0/w_z)^2$, line 1; $16(z_{\text{cm}}/w_z)^2$, line 2; $16(z_{\text{max}}/w_z)$, line 3, where w_z = base width. Note that line 1 is straight.

This analysis unfortunately ignores the content of solute in the stationary phase. Since the isotherm is non-linear the quantity of solute in the stationary phase is not exactly proportional to that in the mobile phase. Accordingly the peak width does not increase exactly in proportion to $\sqrt{z_0}$.

The total quantity of solute in the $R\Delta$ peak is obtained as follows: eqn. 17 is first recast as

$$C_s = \frac{C_m}{R_{F_0}} \left\{ \psi - (\beta C_m) + \frac{4}{3}(\beta C_m)^2 - 2(\beta C_m)^3 \ldots . \right\} \tag{29}$$

where $\beta = \psi\alpha$. The total concentration within the peak at any cross section is

$$C = C_m + C_s \tag{30}$$

and the quantity within the peak is

$$Q = \int C \, dz \tag{31}$$

The distance z is given by

$$z = z^{\ominus} R_F = z^{\ominus} R_{F_0} (1 + 2\beta C_m) = z_0(1 + 2\beta C_m) \tag{32}$$

Where $z^{\ominus}$is the distance moved by the unretained solute or solvent front. Insertion of eqn. 32 into eqn. 31 gives

$$Q = 2\int_0^{C_m^*} (C_m + C_s) \, z^{\ominus} R_{F_0} \beta \, dC_m \tag{33}$$

where C_m^* is the maximum concentration in the mobile phase at the front of the peak. Insertion of eqn. 29 for C_s followed by integration yields

$$Q = \frac{z^{\ominus}}{\beta}(\beta C_m^*)^2 \left\{ 1 - \frac{2}{3}(\beta C_m^*) + \frac{2}{3}(\beta C_m^*)^2 - \frac{4}{5}(\beta C_m^*)^3 + \ldots . \right\} \tag{34}$$

As $z^{\ominus}$increases the peak migrates along the column and z_0, the distance moved by the low concentration tail, increases in proportion.

Since Q is constant C_m^* decreases as $z^{\ominus}$increases and can be found from eqn. 34 by iteration as a function of $z^{\ominus}$or z_0. The peak width from eqn. 32 is $2\beta C_m^* z_0$. N is then obtained finally as

$$N = q\left(\frac{z}{2\beta C_m^* z_0}\right)^2 \tag{35}$$

Again z in eqn. 35 may be chosen as z_0, the position of the low concentration tail, z_{cm}, the position of the centre of mass of the peak, or z_{max} the position of the peak maximum. For a Gaussian peak the multiplier q is 16, for a triangle q is close to 18.

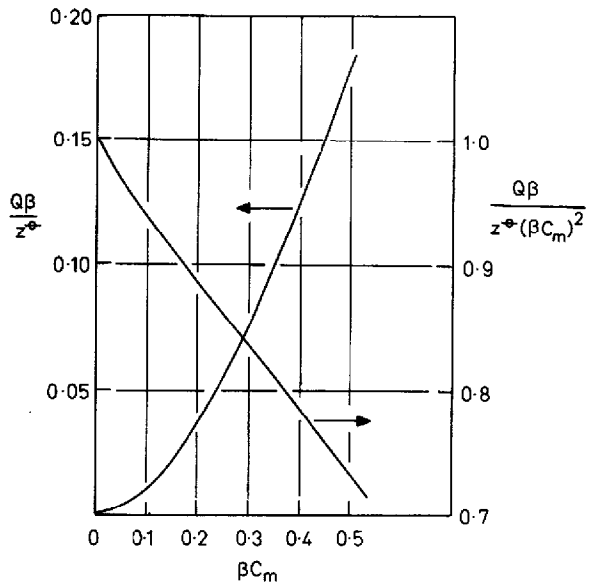

Fig. 11. Relevant parameters from eqn. 34 as a function of βC_m.

In reality peaks will show broadening partly from kinetic effects and partly from thermodynamic effects and we shall therefore use the approximation $q = 16$ throughout.

Fig. 11 shows plots relevant to eqn. 34. Fig. 12 revises Fig. 10 to accommodate the solute in the stationary phase. Fig. 12 shows that the initial curvatures of the upper lines of Fig. 10 are now reduced and that the plot of N *versus* z_{cm} has become an almost perfect straight line.

It may therefore be concluded that for peaks with an $R\Lambda$ profile the plate count

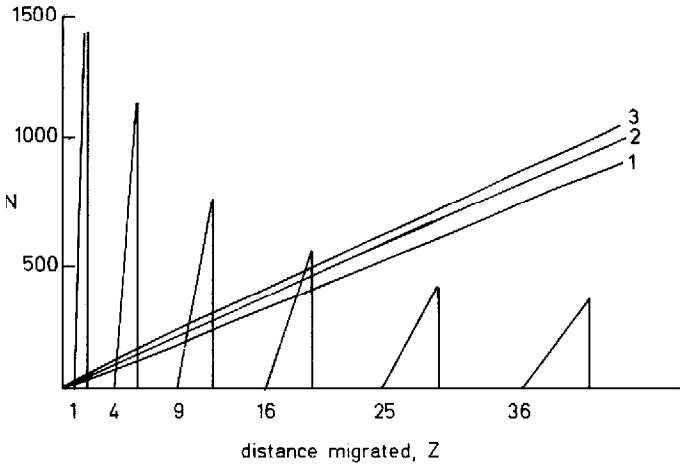

Fig. 12. As for Fig. 10 except that quantity of solute in stationary phase taken into account assuming $k_0 = 4$ and $\alpha = 1$. Note that line 2 is now straight.

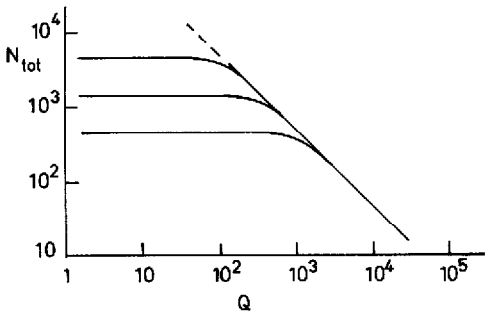

Fig. 13. Effect of load Q (arbitrary units) on number of theoretical plates to which column is equivalent.

for thermodynamic broadening is proportional to column length and that the HETP for this kind of dispersion is a constant independent of the column length.

EFFECT OF QUANTITY INJECTED ON THE NUMBER OF THEORETICAL PLATES FOR *RΔ* PEAK PROFILES

At the column outlet, if reasonable resolution of a solute peak is maintained, βC_m^* at the outlet will not exceed 0.2. For $\beta C_m^* = 0.2$, the polynomial within the brackets in eqn. 34 has the value of 0.89 (see Fig. 11). Accordingly, within this limit, the peak width $2\beta C_m^* z_0$ is proportional to $Q^{\frac{1}{2}}$ with a maximum error of $5\frac{1}{2}\%$. The contribution to H from sample load according to eqn. 26 is thus proportional to Q being given using the approximate form of eqn. 34 by

$$H_{th} = \frac{1}{16}\frac{(2\beta C_m^* z_0)^2}{z} = \frac{1}{16}\frac{(2z_0)^2}{z}\left\{\frac{\beta R_{F_0}}{z_0}\right\}Q$$
$$= \frac{1}{4}(\beta R_{F_0})Q \quad \text{(making the approximation } z = z_0\text{)} \tag{36}$$

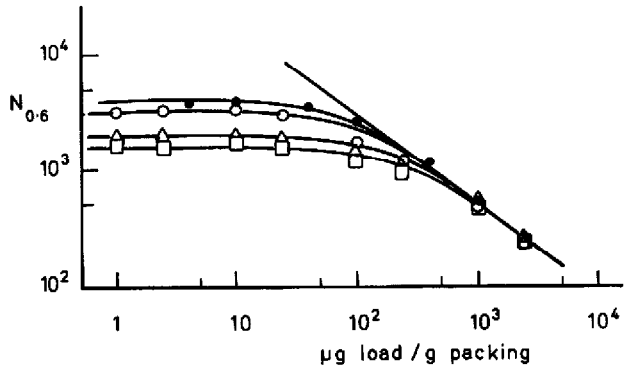

Fig. 14. Practical illustration of effect of load on plate number after de Jong *et al.*[14]. Solute, 2,4-dimethylphenol ($k_0 = 3$). Columns and linear velocities: ●, 100 × 10.8 mm I.D., 5.8 μm, 2.1 mm/s; ○, △, □, 1000 × 10 mm I.D., 20–25 μm, 1.8, 5.5 and 8.4 mm/s respectively. Packing, LiChrosorb SI60; eluent, dichloromethane. Plate height measured using width at 60% of peak height.

The thermodynamic plate height is then determined only by the isotherm curvature parameter α or β, which amounts to the same thing, the retention ratio of the zero concentration sample, R_{F_0}, and the sample quantity Q.

The plate number is then given by

$$N = \frac{L}{H_{\text{total}}} = \frac{L}{\left\{H_0 + \left(\frac{\beta R_{F_0}}{4}\right) Q\right\}} \tag{37}$$

Illustrative plots of log N against log Q are shown in Fig. 13. These plots may be compared with those obtained experimentally by de Jong *et al.*[14,22], an example of which is shown in Fig. 14. The striking similarity of the plots in the two figures gives encouraging support to the theory proposed here.

MAXIMISATION OF THROUGHPUT FOR PEAKS WITH *RA* PROFILE UNDER PRESSURE LIMITED OPERATION: OPTIMUM COLUMN CONFIGURATIONS

The first practical step in any optimisation procedure is to achieve maximum resolution at the analytical level for those solutes which one requires to isolate. It is then possible to calculate the minimum number of theoretical plates required to provide adequate resolution at the preparative level when the spaces between such solutes are fully closed by overload (see Fig. 3). We denote this number by N^*.

We now assume that preparative packings are available with a range of particle sizes having the same retentive characteristics as the packing used for the test analytical separation. The concept of the isochronic column set is now introduced (see ref. 26). Isochronic columns possess the same reduced length $\lambda = L/d_p$ and give the same elution times, t_m, for an unretained solute when using the same pressure drop, Δp, the same eluent (viscosity, η) and the same packing density (described by the column resistance factor φ). This elution time, t_m, is

$$t_m = \frac{\varphi \eta}{\Delta p} \lambda^2 \tag{38}$$

We define the throughput of any column as

$$T = Q/t_m \tag{39}$$

The practical throughput is defined as

$$PT = Q/t_{\text{cycle}} \tag{40}$$

where t_{cycle} is the cycle time for repeated injections. Often t_{cycle} will be expressed as

$$t_{\text{cycle}} = t_m (1 + k_f) \tag{41}$$

where k_f is the capacity factor for the termination of the cycle. Since the cycle time will normally have to be decided by separate considerations we consider first optimisation of T.

For convenience we express the kinetic plate height as

$$H_0 = d_p\, h(v) \tag{42}$$

where $h(v)$ is the reduced plate height at a reduced velocity v. The reduced velocity is defined as

$$v = \frac{L}{t_m}\frac{d_p}{D_m} \tag{43}$$

where D_m is the diffusion coefficient of solute in eluent and $L/t_m = u$, the linear eluent velocity. Replacing t_m by its value from eqn. 38 gives

$$v = \frac{\Delta P\, {d_p}^2}{D_m\, \varphi\eta\lambda} \tag{44}$$

We simplify eqn. 36 to

$$H_{th} = \gamma Q; \qquad \gamma = \frac{\beta R_{F_0}}{4} \tag{45}$$

Giving from eqn. 10

$$H_{total} = d_p\, h(v) + \gamma Q \tag{46}$$

whence using eqn. 39 and $H_{total} = L/N^*$

$$\gamma T = \left\{\frac{\lambda}{N^*} - h(v)\right\}\frac{d_p}{t_m} \tag{47}$$

elimination of t_m between eqns. 47 and 38 gives

$$\gamma T = \left\{\frac{\lambda}{N^*} - h(v)\right\}\frac{d_p \Delta p}{\lambda^2 \varphi\eta} \tag{48}$$

Eqn. 48 shows, in broad terms, that if kinetic dispersion can be ignored, the larger d_p the greater the throughput when λ is kept constant. However, as d_p is increased at constant λ the linear elution velocity increases as d_p and the reduced velocity as ${d_p}^2$. Since $h(v)$ depends upon v according to the widely accepted eqn. 49 (ref. 27)

$$h = \frac{B}{v} + Av^{1/3} + Cv \tag{49}$$

(where typical values for A, B and C are 1, 2 and 0.1 respectively) h will increase strongly for the isochronic set as d_p increases. A stage must then be reached when the $h(v)$ term in eqn. 48 begins to dominate the throughput and eventually reduces it as d_p is increased. This will normally occur when v is large and we can approximate $h(v)$ by

$$h = Cv \qquad \text{with } C \cong 0.1 \tag{50}$$

Inserting eqns. 44 and 50 into eqn. 48 gives

$$\gamma T = \left\{\frac{1}{N^*} - \frac{C\,\Delta p\,{d_p}^2}{D_m\,\varphi\eta\,\lambda^2}\right\}\frac{\Delta p}{\varphi\eta}\frac{d_p}{\lambda} \tag{51}$$

Differentiating γT with respect to (d_p/λ) and setting the differential to zero gives the value of d_p/λ for maximum throughput

$$\left(\frac{d_p}{\lambda}\right)_{opt} = \left(\frac{{d_p}^2}{L}\right)_{opt} = \left\{\frac{D_m\,\varphi\eta}{3N^*C\Delta p}\right\}^{\frac{1}{2}} \tag{52}$$

Insertion of this value for d_p/λ into eqn. 51 gives

$$\gamma T_{opt} = \frac{2}{3N^*}\left\{\frac{\Delta p\,D_m}{3\,\varphi\eta\,N^*C}\right\}^{\frac{1}{2}} \tag{53}$$

Under these conditions it is readily shown that the kinetic dispersion is one half of the thermodynamic dispersion.

The reduced velocity at which the optimum throughput is obtained is found by substituting eqn. 52 into eqn. 44 to eliminate d_p giving

$$\nu_{opt} = \frac{1}{3}\left(\frac{\lambda}{N^*C}\right) \tag{54}$$

Under typical conditions λ might be 20000 and N^* between 50 and 2000; taking $C = 0.1$, ν_{opt} will then lie between 33 and 1333. We can now check on the validity of approximation 50 by first expressing the reduced plate height given by eqn. 49 in the alternative forms

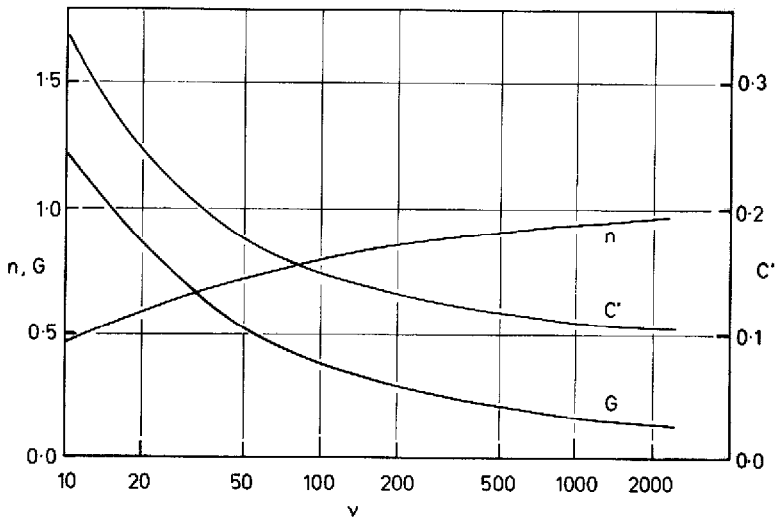

Fig. 15. Dependence of C', n and G (eqns. 55 and 56) upon reduced velocity, ν.

$$h = C'v \tag{55}$$

$$h = Gv^n \tag{56}$$

where C', G and n are now weak functions of v. Values of C', G and n as functions of v are shown in Fig. 15. Typical values of C' are 0.20 at $v = 33$ and 0.108 at $v = 1333$. It is thus clear that the approximation $C = 0.1$, eqn. 50, is poor at low values of v. The use of eqn. 55 with the correct value of C' provides a much closer approximation to the true optimum conditions but C' can only be found by successive approximation using eqns. 52 and 54 for specified values of λ and N^*. Iteration is initiated by taking $C = 0.1$ as the first value. Alternatively the better approximation (eqn. 56) can be used but eqns. 52–54 must now be replaced by

$$\frac{d_p}{\lambda} = \left\{\frac{\lambda}{(2n+1)N^*}\right\}^{\frac{1}{2n}} \left\{\frac{D_m \varphi \eta}{G \Delta p \lambda}\right\}^{\frac{1}{n}} \tag{57}$$

$$\gamma T_{opt} = \left\{\frac{2n}{(2n+1)N^*}\right\} \left\{\frac{\lambda}{(2n+1)N^*}\right\}^{\frac{1}{2n}} \left\{\frac{\Delta p D_m}{G \varphi \eta \lambda}\right\}^{\frac{1}{n}} \tag{58}$$

$$v_{opt} = \frac{1}{G} \left\{\frac{\lambda}{(2n+1)N^*}\right\}^{\frac{1}{n}} \tag{59}$$

Again iteration is required starting with initial values of $G = 0.1$ and $n = 1$ corresponding to approximation 50.

The three methods of estimating optimum conditions are compared in Figs. 16 and 17 for columns with a fixed reduced length $\lambda = 20000$.

Method a is based upon eqns. 52–54 with $C = 0.1$; method b is based upon eqns. 52–54 using values of C' found by iteration and method c is based upon eqns. 57–59 using values of G and n found by iteration.

The other operating parameters are assumed to have the values: $\Delta p = 2 \cdot 10^7$ N m^{-2} (200 bar), $D_m = 1.0 \cdot 10^{-9}$ m^2 s^{-1}, $\varphi = 1.0 \cdot 10^3$ and $\eta = 1.0 \cdot 10^{-3}$ N s m^{-2}. Plate height eqn. 49 with $B = 2$, $A = 1$ and $C = 0.1$, values of C', G and n as shown in Fig. 14.

Figs. 16 and 17 confirm that there is good agreement between the calculations for methods b and c but show that even method a gives reasonable approximations to d_p and T_{opt}.

An important feature of eqn. 53 is that the optimum throughput does not apparently depend upon either λ or d_p. These parameters only enter into the optimal conditions through eqn. 52 which specifies the ratio d_p/λ for optimum throughput. It thus appears that the optimum throughput can be achieved with a wide range of geometrical configurations. This conclusion is slightly modified when we recognise that C is not a true constant and ought to be replaced by C', or alternatively that the more precise eqn. 58 should be used. In this equation T is seen to be proportional to $\lambda^{(1+n)/2n}$. Since n is close to unity, T depends rather weakly upon λ in the sense that larger λ gives higher T until λ is so large that in the limit n becomes unity. Thus λ does have to have a large enough value for near maximum T to be obtained.

TABLE I

VARIOUS OPTIMUM CONDITIONS FOR PLC

Assumed parameters: $\Delta p = 200$ bar $= 2 \cdot 10^7$ N m^{-2}; $D_m = 1.0 \cdot 10^{-9}$ m^2 s^{-1}; $\eta = 1 \cdot 10^{-3}$ N s m^{-2}; $\theta = 1000$, $h = 2/v + v^{1/3} + 0.1v$; $h = C'v = Gv^n$

N^*	$\lambda = 20000$					$L = 500$ mm					$d_p = 20\ \mu$m				
	d_p (μm)	L (mm)	C'	v	γT (m s^{-1})	d_p (μm)	$\lambda/1000$	C'	v	γT (m s^{-1})	L (mm)	$\lambda/1000$	C'	v	γT (m s^{-1})
50	35	700	0.108	1240	$4.6 \cdot 10^{-4}$	30	17	0.109	1040	$4.7 \cdot 10^{-4}$	240	12	0.113	690	$4.6 \cdot 10^{-4}$
100	24	480	0.114	580	$1.6 \cdot 10^{-4}$	25	20	0.114	600	$1.6 \cdot 10^{-4}$	340	17	0.116	480	$1.6 \cdot 10^{-4}$
200	16	320	0.124	270	$5.5 \cdot 10^{-5}$	20	25	0.122	350	$5.5 \cdot 10^{-5}$	480	24	0.121	333	$5.5 \cdot 10^{-5}$
500	9.5	190	0.150	90	$1.3 \cdot 10^{-5}$	16	32	0.135	160	$1.3 \cdot 10^{-5}$	680	39	0.129	205	$1.3 \cdot 10^{-5}$
1000	6.8	140	0.196	35	$3.9 \cdot 10^{-6}$	13	39	0.151	90	$4.4 \cdot 10^{-6}$	980	49	0.138	140	$4.7 \cdot 10^{-6}$
2000	3.2	65	0.330	10	$1.0 \cdot 10^{-6}$	10	48	0.178	50	$1.4 \cdot 10^{-6}$	1400	69	0.150	100	$1.6 \cdot 10^{-6}$

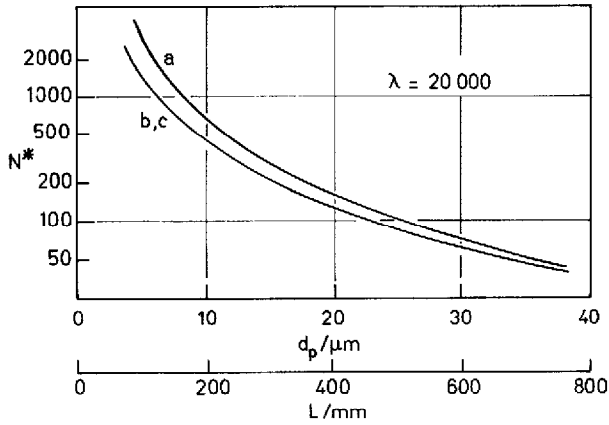

Fig. 16. Dependence of particle diameter, d_p, and column length, L, upon N^* for cases a, b and c (see text), with $\lambda = 20000$.

Nevertheless there is still wide flexibility in the choice of optimum conditions for PLC. Thus if λ is fixed, d_p will have optimum values for different N^*; if column length L is fixed, d_p will have a different set of optimum values, and if d_p is fixed, λ or L will take optimum values. The values of T and of other parameters for the restrictions $\lambda = 20000$, $L = 500$ mm and $d_p = 20$ μm are compared in Table I. The values are calculated using C' values in place of C in eqns. 52–54. It is clear that the throughput is relatively insensitive to the nature of the restriction imposed and depends primarily upon N^*. The throughput is given in the three cases to a good approximation by

$$\log_{10}\left\{\frac{\gamma\, T_{opt}}{\text{m s}^{-1}}\right\} = -1.58 \log_{10} N^* - 0.64 \tag{62}$$

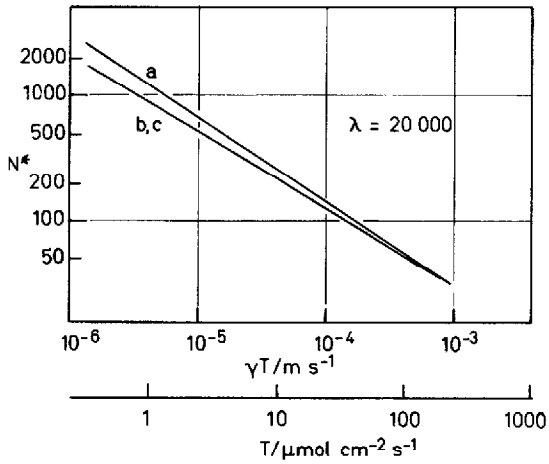

Fig. 17. Dependence of throughput, T, upon N^* for methods a, b and c (see text) with $\lambda = 20000$.

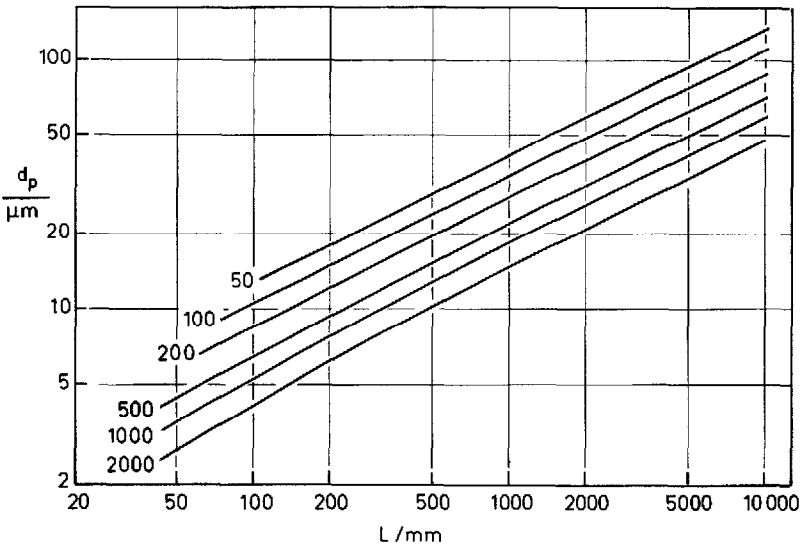

Fig. 18. Optimum combinations of particle size, d_p, and column length, L, for different values of N^* given on lines. Operating parameters as given in Table I.

The slope -1.58 is slightly steeper than the value of -1.5 predicted using constant C (eqn. 54).

Eqns. 53 and 58 for optimised throughput confirm that, as in analytical HPLC, performance can always be improved by (a) increasing pressure drop, Δp; (b) increasing diffusion rate of solute in eluent, D_m; (c) decreasing eluent viscosity, η, and (d) decreasing the column flow resistance factor, φ.

In practice it will be desirable to have available a range of both column lengths and particle diameters so that appropriate optimal combination can be selected for particular preparative applications.

The range of choice of L, λ and d_p for optimum conditions with different N^* requirements is summarised in Fig. 18. The calculations use method b with values of C' found by iteration for particular λ and N^* values. For each N^* the appropriate T is given to a good approximation by eqn. 62. Since there is little dependence of throughput upon any parameter other than N^* one is free to choose the most appropriate combination of L and d_p consistent with the desired N^* value. The choice may well be determined by a desire to avoid columns which are short and wide and will present problems of distribution of sample to the column cross section. Other considerations in practice may be the relative costs of say 5- and 20-μm materials or the available lengths of preparative scale columns. It is also likely that as the scale of the preparation increases there will be a tendency to use altogether larger systems, that is wider and longer columns packed with larger particles but keeping the d_p/λ ratio at the appropriate value for maximum throughput.

NUMERICAL ESTIMATION OF OPTIMUM PRACTICAL THROUGHPUT

In order to estimate the throughput (see eqns. 39 and 40) which might be

achieved in practice it is necessary first to evaluate $\gamma = \beta R_{F_0}/4$ which occurs as the multiple of throughput in eqns. 54 and 59. Rewriting in terms of k_0 we obtain

$$\gamma = \frac{1}{4}\left\{\frac{k_0}{(1+k_0)^2}\right\}\alpha \tag{63}$$

We now require to estimate α, the curvature of the isotherm. Assuming that a Langmuir isotherm applies, elementary adsorption theory given for the fractional coverage of an adsorbent surface, θ,

$$\theta = \frac{KC_m}{1+KC_m} \tag{64}$$

where K is the ratio of the adsorption to desorption rate constants. θ may be expressed as C_s/C_s^∞ where C_s^∞ is the saturation monolayer coverage of the adsorbent. Thus

$$C_s = \frac{KC_s^\infty\, C_m}{1+KC_m} \tag{65}$$

Identifying with the Langmuir isotherm as expressed by eqn. 12 we obtain

$$k_0 = KC_s^\infty, \qquad \alpha = K \qquad \text{and} \qquad k_0/\alpha = C_s^\infty \tag{66}$$

whence

$$\alpha = k_0/C_s^\infty \tag{67}$$

Substituting for α into eqn. 63 then gives

$$\gamma = \frac{1}{4}\left\{\frac{k_0}{1+k_0}\right\}^2 \frac{1}{C_s^\infty} \tag{68}$$

The final requirement is to estimate C_s^∞. Most HPLC bonded materials show coverages of bonded phase in the region of *ca.* 3 μmol m^{-2} and a typical silica gel will have a specific surface area of around 200 m^2 g^{-1} with a packed bed density of about 0.7 g cm^{-3}. The content of bonded phase is thus around 400 μmol cm^{-3}. It would not be unreasonable to take a value of this order for C_s^∞. Taking $k_0 = 4$ and $C_s^\infty = 400$ μmol cm^{-3} gives $\gamma = 4 \cdot 10^{-4}$ μmol^{-1} cm^3 $= 4 \cdot 10^{-4}$ mol^{-1} m^3.

Eqn. 62 with appropriate change of units then takes the form:

$$\log_{10}\left\{\frac{T_{opt}}{\mu\text{mol cm}^{-2}\text{ min}^{-1}}\right\} = 6.54 - 1.58 \log N^* \tag{69}$$

Supposing finally that the solute has molecular weight of 200 g mol^{-1}, the practical throughput, PT (eqn. 40) taking $k_f = k_0 + 1$, is then given by

TABLE II

SAMPLE DILUTION AT COLUMN OUTLET IN PLC

Conditions as specified for Table I, $k_f = 5$.

N^*	PT ($g\ cm^{-2}\ h^{-1}$)	$\lambda = 20000$			$L = 500$ mm			$d_p = 20\ \mu m$		
		d_p (μm)	Cycles (h^{-1})	Mean conc.* (g/l)	d_p (μm)	Cycles (h^{-1})	Mean conc.* (g/l)	L (mm)	Cycles (h^{-1})	Mean conc.* (g/l)
50	14	35	30	3.0	30	41	3.0	240	90	2.6
100	4.8	24	30	2.0	25	30	2.0	340	43	2.0
200	1.6	16	30	1.5	20	19	1.5	480	21	1.4
500	0.38	9.5	30	0.9	16	12	0.9	800	8	0.9
1000	0.13	6.8	30	0.6	13	8	0.6	1000	5	0.5
2000	0.042	3.2	30	0.5	10	5	0.5	1400	2.5	0.35

* Mean concentration is amount collected divided by base peak volume.

$$\log_{10}\left\{\frac{PT_{opt}}{\text{g cm}^{-2}\text{ h}^{-1}}\right\} = 3.84 - 1.58 \log N^* \quad (70)$$

Typical values of PT are then 0.13 g cm^{-2} h^{-1} at $N^* = 1000$ and 14 g cm^{-2} h^{-1} at $N^* = 50$.

Eqn. 38 gives t_m for a set of isochronic columns with $\lambda = 20000$ as 20 s. The run time is therefore 6×20 s $= 2$ min. Thus using the isochronic set it would be necessary to carry out 30 injections per hour. If N^* were 1000 then each injection would be of about 4 mg whereas with $N^* = 50$ then 0.5 g per run for each cm^2 of column section.

A major factor in any chromatographic separation is sample dilution. This is particularly relevant in PLC where it will be necessary in most cases to isolate the separated materials from eluent. It is a straightforward matter to calculate the mean sample concentration in collected eluent for the various cases considered in Table I. The results are shown in Table II which gives the concentrations of sample eluted at with $k_0 = 4$ when collection is taken over the base peak width. The insensitivity of the collected concentration to the exact geometry of the column is again most notable. Surprisingly there is rather little loss of concentration when long columns with relatively large particles are used for quite high efficiency separations (last entry Table II). Nevertheless Table II emphasises that the maximum concentrations which can be expected in PLC at the column outlet range from some 0.3 to 3 g/l as N^* decreases from 2000 to 50.

On the broad subject of cost of separating materials by PLC, it is clear that both column packing materials and eluents must be of the highest quality. A given weight of packing material will process between 1–10% of its own weight of solute per hour; and a given yield of purified solute will require between 5000 and 300 times its own weight or volume of eluent for elution. Thus only materials with a value of say 1000–10000 times that of common bulk organic chemcials can be candidates for production LC. Minimum production costs in PLC are thus likely to be in the range of \$1 to \$10 per gram, similar to those of high-grade chromatographic packing materials even if the capital cost of the equipment is discounted.

CONCLUSIONS AND LIMITATIONS

(1) For many sorbent–eluent combinations the distribution of a solute follows a Langmuir type isotherm up to concentrations where deviation from linearity is around 20%. Under these circumstances the peak profile is very close to triangular.

(2) Under these conditions there will inevitably be some interference between competing solutes. Such interferences cannot be predicted or dealt with simply and have been ignored in our treatment. Their effect is likely to be secondary especially if solutes are fairly well separated (large α values).

(3) With triangular peak profiles the peak base width, in the absence of kinetic dispersion, increases with the square root of the distance migrated. Accordingly optimisation can be carried out using similar procedures to those employed in optimising kinetic performance.

(4) Optimisation for maximum throughput under conditions of restricted pres-

sure drop requires a balancing of kinetic and thermodynamic dispersion. The theoretical analysis shows that maximum throughput occurs when the kinetic dispersion is half the thermodynamic dispersion.

(5) The maximum throughput, T_{opt}, is determined almost exclusively by the minimum number of theoretical plates which provides acceptable resolution of the components of interest N^*. It also depends upon the operating parameters: pressure drop, solute diffusion coefficient, eluent viscosity and column resistance parameter.

(6) For typical values of operating parameters, assuming a Langmuir isotherm and a molecular weight of 200 g mol^{-1}, it is found that the maximum practical throughput, defined as injected quantity/elution time of solute with $k_0 = 5$ is given by

$$\log_{10}\left\{\frac{PT}{\text{g cm}^{-2}\text{ h}^{-1}}\right\} = 3.84 - 1.58 \log N^*$$

(7) Optimum throughput is obtained for a specific ratio of d_p^2/L which depends upon N^* and the operating parameters. For a given N^* there is a wide range of d_p and L which give the same N^*.

(8) The optimum throughput for a given N^* is obtained for a specific ratio of d_p^2/L and is almost independent of the actual values of d_p and L.

(9) Likewise sample dilution for optimum conditions for a given N^* is independent of the actual values of d_p and L.

(10) It is recognised that the whole of the above treatment makes major assumptions about the nature of the partition isotherm of a typical solute and ignores interferences of solutes which could produce distortion of isotherms. We do, however, claim that the broad results provide a useful and realistic framework for optimising throughput in preparative liquid chromatography.

GLOSSARY OF SYMBOLS

A	constant in plate height eqn. 49, value 1
A_m	cross sectional area of eluent in column
B	constant in plate height eqn. 49, value 2
C	constant in plate height eqn. 49, value 0.1
C'	constant in modified plate height eqn. 55
C	concentration: total amount of solute per unit volume of column bed
C_m, C_s	concentrations: amount of solute in eluent phase, and stationary phase per unit volume of column bed
C_0	initial concentration of solute in column immediately following injection
C_m^*	maximum concentration of solute in mobile phase in a chromatographic band
C_s^∞	concentration of solute in stationary phase corresponding to monolayer coverage on adsorbent per unit volume of column bed
D_m	diffusion coefficient of solute in eluent
d_p	mean particle diameter
G	constant in modified plate height eqn. 56
H	plate height

H_0	kinetic contribution to plate height corresponding to an analytical sample
H_{th}	thermodynamic contribution to plate height
H_{total}	total plate height
h, $h(v)$	reduced plate height, value of h at specified reduced velocity
k	column capacity ratio
k_0	column capacity ratio at zero concentrations of solute
k_{C_m}	column capacity ratio for a concentration C_m in tail of a peak
k_{front}	column capacity ratio for a front
k_f	column capacity ratio corresponding to end of cycle in a series of repetitive PLC runs
K	equilibrium distribution coefficient for an adsorbent
L	column length
N	plate number
N^*	minimum number of plates required to provide adequate resolution in a preparative run
n	constant in modified plate height eqn. 56
Δp	pressure drop
PT, PT_{opt}	practical throughput, optimum practical throughput
Q	quantity injected
q	configurational factor (in eqn. 35)
R_F, R_{F_0}	retention ratio, and retention ratio at zero concentration of solute
T, T_{opt}	throughput and optimum throughput
t_m	elution time of unretained solute
t_{cycle}	cycle time in PLC
u	eluent linear velocity
V_{inj}	volume of injected sample
V_{R1}, V_{R2}	retention volumes of solutes 1 and 2
V_m	volume of eluent phase in column
V_s	volume of stationary phase in column
w_z	base peak width measured as a distance within the column
x, X	dummy variables
z	distance from start of column
Δz	distance measured from centre of mass of peak
z_0	distance migrated by low concentration side of peak
$z^{\ominus}$	distance migrated by unretained solute or solvent front
z_{cm}	distance migrated by centre of mass of peak
z_{max}	distance migrated by maximum concentration in peak
z_{inj}	length of column occupied by peak immediately following injection
α	parameter in Langmuir isotherm, relative retention ratio
β	parameter given by $\alpha k_0/(1+k_0)$
γ	constant relating plate height to Q
η	eluent viscosity
θ	fractional surface coverage
λ	reduced column length, L/d_p
ν, ν_{opt}	reduced eluent velocity, optimum reduced velocity
φ	column flow resistance factor
ψ	constant $k_0/(1+k_0)$

σ, σ_z standard deviation of peak measured as elution volume and as distance in column

REFERENCES

1 J. H. Knox and M. Saleem, *J. Chromatogr. Sci.*, 7 (1969) 614–622.
2 J. H. Knox and M. T. Gilbert, *J. Chromatogr.*, 186 (1979) 405–418.
3 I. Halàsz, H. Schmidt and P. Vogtel, *J. Chromatogr.*, 126 (1967) 19–33.
4 L. R. Snyder, *J. Chromatogr. Sci.*, 15 (1977) 441–449.
5 G. Guiochon, in Cs. Horváth (Editor), *High Performance Liquid Chromatography*, Vol. 2, Academic Press, New York, London, 1980, pp. 1–56.
6 R. Rosset, M. Caude, J. Desbarres and E. Schmidt, *Analusis*, 8 (1980) 213–223.
7 K. P. Hupe and H. H. Lauer, *J. Chromatogr.*, 203 (1981) 41–52.
8 C. N. Reilley, G. P. Hildebrand and J. W. Ashley, Jr., *Anal. Chem.*, 34 (1962) 1198.
9 B. Coq, G. Cretier and J. L. Rocca, *J. Chromatogr.*, 186 (1979) 457.
10 R. P. W. Scott and P. Kucera, *J. Chromatogr.*, 119 (1976) 467.
11 R. A. Barford, R. McGraw and H. L. Rothbart, *J. Chromatogr.*, 166 (1978) 365–372.
12 P. C. Haarhoff and H. J. van der Linde, *Anal. Chem.*, 38 (1966) 573.
13 J. F. K. Huber and R. G. Gerritse, *J. Chromatogr.*, 58 (1971) 137.
14 A. W. J. de Jong, H. Poppe and J. C. Kraak, *J. Chromatogr.*, 209 (1981) 432–436.
15 J. H. Knox and R. Kaliszan, *J. Chromatogr.*, 349 (1985) 211–234.
16 G. Cretier and J. L. Rocca, *Chromatographia*, 18 (1984) 623–627.
17 H. Poppe and J. C. Kraak, *J. Chromatogr.*, 255 (1983) 395.
18 A. W. J. de Jong, J. C. Kraak, H. Poppe and F. Nooitgedacht, *J. Chromatogr.*, 193 (1980) 181–185.
19 B. Coq, G. Cretier and J. L. Rocca, *Anal. Chem.*, 54 (1982) 2271–2277.
20 F. Eisenbeiss, S. Ehlevding, A. Wehrli and J. F. K. Huber, *Chromatographia*, 20 (1985) 657–663.
21 J. C. Smit, H. C. Smit and E. M. de Jaeger, *Anal. Chim. Acta*, 122 (1980) 1.
22 A. W. J. de Jong, H. Poppe and J. C. Kraak, *J. Chromatogr.*, 148 (1978) 127–141.
23 R. A. Wall, *J. Liq. Chromatogr.*, 2 (1979) 775–798.
24 H. M. Pyper and J. H. Knox, *Ph.D. Thesis*, University of Edinburgh, 1984.
25 P. Gareil, L. Personnaz, J. P. Feraud and M. Caude, *J. Chromatogr.*, 192 (1980) 53–74.
26 J. H. Knox, in C. F. Simpson (Editor), *Techniques in Liquid Chromatography*, Wiley, London, New York, 1982, p. 31.
27 J. H. Knox, *J. Chromatogr. Sci.*, 15 (1977) 352.